

Communication

Rapid Magnetic Susceptibility Characterization of Coastal Morphosedimentary Units at Two Insular Strandplains in Estonia

Ilya V. Buynevich ^{1,*} , Hannes Tõnisson ², Alar Rosentau ³ , Tiit Hang ³ , Are Kont ², Toru Tamura ⁴, Sten Suuroja ⁵, Valdeko Palginõmm ² and Sophia F. S. Döring ⁶

¹ Department of Earth and Environmental Science, Temple University, 1901 N 13th St., Philadelphia, PA 19122, USA

² Institute of Ecology, Tallinn University, 10120 Tallinn, Estonia

³ Institute of Ecology and Earth Sciences, University of Tartu, 50409 Tartu, Estonia

⁴ Geological Survey of Japan (AIST), Tsukuba, Central 7, 1-1-1, Higashi, Tsukuba 305-8567, Japan

⁵ Geological Survey of Estonia, 12618 Tallinn, Estonia

⁶ Hochschule Bremen, 28199 Bremen, Germany

* Correspondence: coast@temple.edu

Abstract: Coastal archives of changing hydrometeorological conditions include mineralogical anomalies, such as heavy-mineral concentrations (HMCs) of variable thickness and intensity, which contain varying ferrimagnetic (e.g., magnetite) fractions. As an effective alternative to laborious mineralogical and granulometric analysis, we present the first set of bulk-volume low-field magnetic susceptibility (MS) databases from beach and dune lithosomes in the Western Estonian archipelago: Harilaid cusplate foreland (westernmost Saaremaa Island) and Tahkuna strandplain (northernmost Hiiumaa Island). Readings were conducted both *in situ* from trench walls and on core subsamples. At the Tahkuna site, late Holocene beach ridges reveal substantially lower values: quartz-dominated dune sequences grade from 5–20 μSI downward to diamagnetically dominated (-1 – -7 μSI) beach facies. Values are higher (20–140 μSI) in historically reactivated parabolic dunes that are encroaching southward over the strandplain. At the Harilaid site, four beach dune ridges (height: 2–3 m) that span the past 250–300 years show a general increase in mean MS from 320–850 μSI with decreasing age, with peaks of 1000–2000 μSI below the dune crests (depth: ~ 0.3 – 0.6 m) likely related to contemporary wind acceleration during ridge aggradation. The highest mineralogical anomalies range from 2000–5500 μSI in the historic dune sections and exceed 8000 μSI along the actively eroding upper-berm segments, typical of HMCs generated by moderate storms. MS anomalies are likely correlated with high-amplitude electromagnetic signal responses in georadar records and provide useful information for optical luminescence sampling strategies. Our study demonstrates that magnetic susceptibility trends provide a useful means of rapidly assessing relative temporal changes in overall wave/wind climates, help identify and correlate discrete anomalies related to extreme events, serve as local beach/dune boundary indicators, and represent potentially quantifiable paleo-energy indices.

Keywords: storm; morphostratigraphy; magnetite; paramagnetic; georadar



Citation: Buynevich, I.V.; Tõnisson, H.; Rosentau, A.; Hang, T.; Kont, A.; Tamura, T.; Suuroja, S.; Palginõmm, V.; Döring, S.F.S. Rapid Magnetic Susceptibility Characterization of Coastal Morphosedimentary Units at Two Insular Strandplains in Estonia. *J. Mar. Sci. Eng.* **2023**, *11*, 232. <https://doi.org/10.3390/jmse11020232>

Academic Editor: Antoni Calafat

Received: 7 December 2022

Revised: 9 January 2023

Accepted: 12 January 2023

Published: 17 January 2023



Copyright: © 2023 by the authors. Licensee MDPI, Basel, Switzerland. This article is an open access article distributed under the terms and conditions of the Creative Commons Attribution (CC BY) license (<https://creativecommons.org/licenses/by/4.0/>).

1. Introduction

Coastal accumulation forms serve as morphological and sedimentary archives of past oceanographic forcings, with beach/dune ridges (strandplains) and reactivated dunes preserving rich archives of long-term wave climates, storm impacts, and near-surface wind activities [1–6]. Reconstructing the signatures of environmental and anthropogenic changes in coastal landscapes is particularly important in a current regime of rapid shifts in climate, sea level, and sediment supply. However, in many siliciclastic beach and dune lithosomes, evidence of past events is often preserved as erosional (discontinuities, density lag) rather

than depositional geoindicators. Textural and stratigraphic data alone are not always adequate for locating and mapping these event signatures, and in this context, lithological anomalies, such as heavy mineral concentrations (HMCs) provide a rich dataset, which (1) is recognized visually in outcrops, trenches, and cores; (2) can be correlated with geophysical data anomalies (georadar reflections); and (3) offers a means of quantitative assessment of the energy conditions responsible for producing a specific anomaly [4,7–10].

To date, however, little research has been carried out to rapidly and effectively assess such anomalies in the field or laboratory as an independent component of coastal stratigraphic and geophysical research [4,11]. Low-field bulk magnetic susceptibility (MS) is emerging as a means of such *in situ* analyses of Holocene beach and aeolian deposits [12–14]. The aim of this study is to assess a new dataset of MS values from two sites along the Estonian archipelago (Tahkuna, Hiiumaa Island and Harilaid, Saaremaa Island; Figure 1) in order to demonstrate the effectiveness of the method as a potential new component of coastal geological research. Rather than an interpretative dataset addressing specific interpretations of hydroclimatic conditions responsible for HMC formation, this paper presents examples of potential MS values encountered in spatially and temporally different settings, having a similar physiographic background.

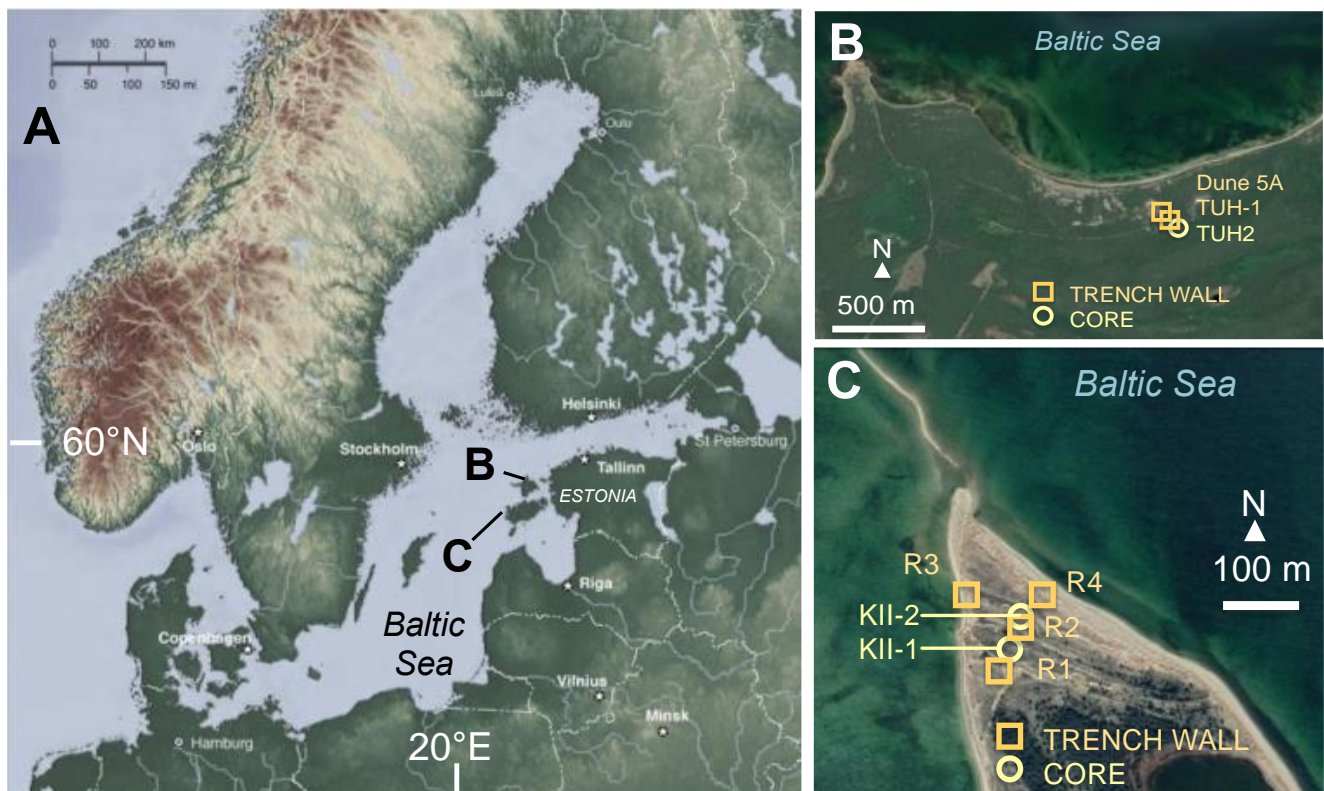


Figure 1. (A) Location of Hiiumaa (B) and Saaremaa (C) Islands along the east coast of the Baltic Sea. (B) Tahkuna strandplain, northern Hiiumaa Island, with locations of a beach ridge trench (Site TUH-1; see Figure 2A), nearby core sample (TUH-2), and a deep trench through a large parabolic dune (Site 5A; Figure 2B). (C) Harilaid strandplain, northwest Saaremaa Island, showing locations of the four trenched ridge generations (trenches R1–4). Cores KII-1 and KII-2 (see Figure 2C) were taken through ridges R1 and R2 (Figure 2D), respectively, with a coastal exposure measured for ridge R3 (see Figure 2E; GoogleEarth™ database).

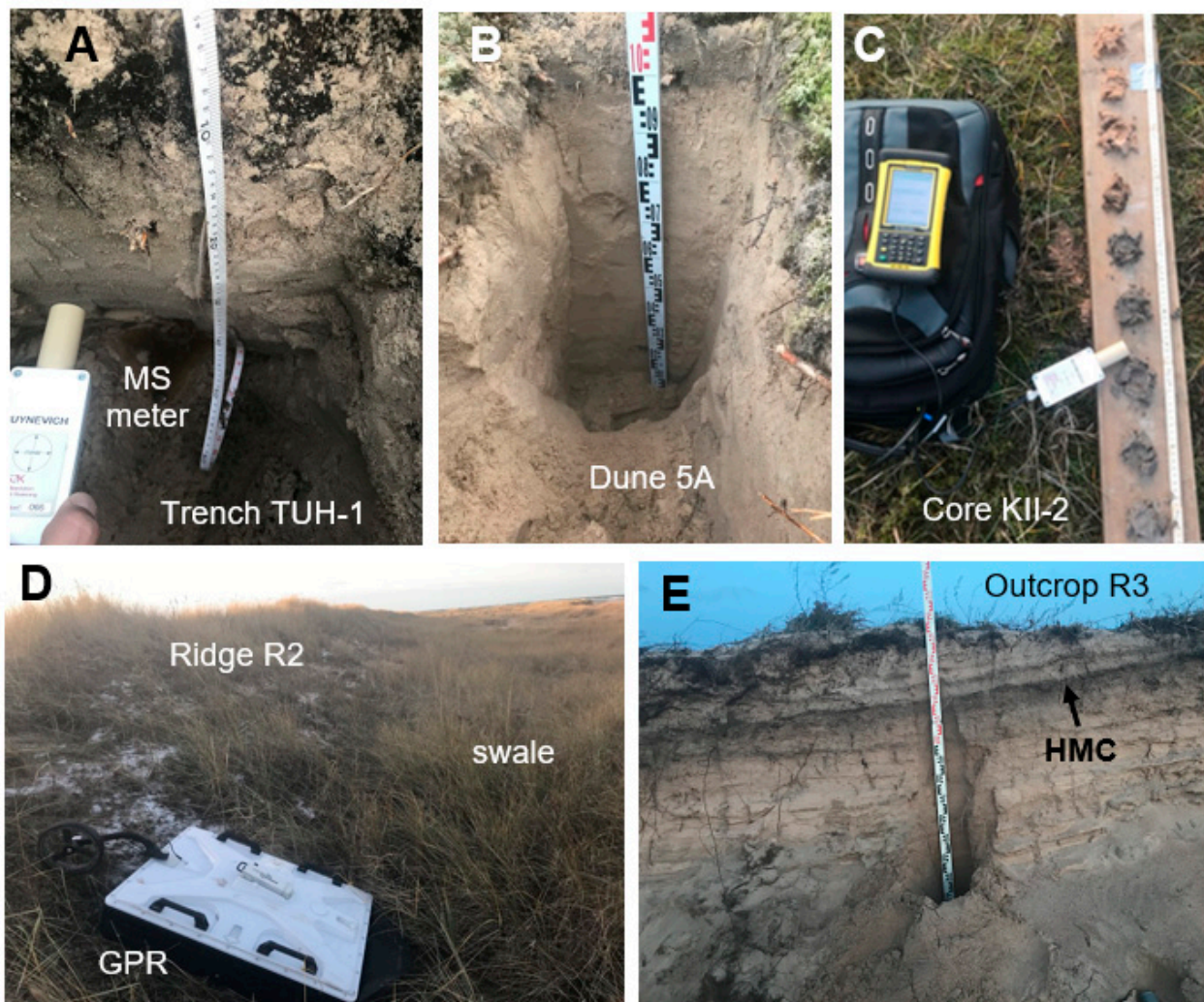


Figure 2. Field photographs of sampled sites on Hiiumaa (A,B) and Saaremaa (C–E) Islands (see Figure 1B,C for locations). (A) A trench through a beach ridge shows well-sorted quartz-rich sand down to a water table at 0.7 m. A Bartington MS2K field sensor was used for *in situ* magnetic susceptibility (MS) measurements. Core TUH-2 was taken landward of the trench. (B) A 1 m deep trench through the top of a high parabolic dune seaward of TUH sites. (C) Samples from a 2.4 m deep core KII-2 (ridge R2) at the Harilaid strandplain arranged on a wooden board showing darker, less oxidized sand with depth (toward the bottom of the photo). The personal digital assistant (PDA) and MS sensor are visible, with MS3 m in the backpack. (D) Ridge 2 and a seaward swale (R2/R3), with a ground-penetrating radar (GPR) antenna (~1 m long) for scale. (E) An erosional scarp reveals the bedding of the upper beach and dune section of ridge R3. Thin paleosol horizons and multiple heavy mineral concentrations (HMC) were measured *in situ*.

2. Study Areas

Study sites are located in the middle section of the Tahkuna peninsula on the Northern Hiiumaa Island (Figure 1B) and Harilaid peninsula, NW Saaremaa Island Figure 1C). The first site is a north-facing coastal strandplain anchored to bedrock headlands, whereas the second is a cusped foreland exposed to both the west (erosional section) and northeast. Over the past two millennia, the coastlines of Estonian islands have been outpacing the regional sea level rise by 2–3 mm/yr (a trend decreasing in a southerly direction) as a response to neotectonic and glacio-isostatic uplift [15–17]. Therefore, the majority of the coastal sedimentary systems have undergone varying rates of uplift during and following their formation [18–21].

This shoreline is functionally tideless, with fair-weather wave heights of <0.5 m. Storm surges (wave height > 2.0 m) and sea ice are the primary drivers of change along many accumulation forms [22–24]. Depositional landforms range from gravel to sand, with the present study concentrated on sandy lithosomes, primarily 1.0–1.2 m high beach/dune ridge sets (Figures 1 and 2). The Harilaid peninsula has been the focus of recent investigations, which demonstrate that the ridges formed within the past 250–300 years and the substantial erosion in the west are the result of intense storms in the 20th century [22,23,25]. One of the most recent impacts was by the winter storm Gudrun in 2005 [26–28].

3. Materials and Methods

This study is part of a regional, multi-institutional geological research effort in December 2019. For assessing the relative magnitude of exposed heavy mineral concentrations (driven primarily by the ferrimagnetic fraction, e.g., magnetite), 170 bulk-volume magnetic susceptibility values were obtained *in situ*. Measurements were made using a portable Trimble® Nomad® 900 handheld computer with a high-sensitivity Bartington® MS3 m. We used the MS2K field scanning sensor (operational frequency: 0.93 kHz) with a sensitivity threshold of 50% at a surface diameter of 2.5 cm (response area) and a response depth of 0.3 cm into the sediment (10% at 0.8 cm) [4]. Due to the response decay with depth, the field sensor is ideal for measuring relative MS values on moderately smooth sediment surfaces, particularly where the sampling of thin HMC horizons is problematic. Most samples in this study had a mean grain size in a medium sand range (0.2–0.5 mm), with microscope analysis indicating that nearly all opaque and non-opaque heavy minerals (density > 2.7 g/cm³) comprise a finer fraction in each sample.

Measurements were made at 5 or 10 cm intervals in trench walls (2 at Tahkuna; 3 trenches and 1 outcrop at Harilaid; Figures 1 and 2A,B,E; Table 1) guided by visible sedimentological variations (heavy mineral concentrations, etc.). At three inter-ridge swale sites, an electric vibrocore with a window sampler was used to extract subsamples, which were laid out at stratigraphic intervals on a wooden board for measurements (one at Tahkuna; two at Harilaid; Figure 2C). In addition, samples were taken from modern beach and dune surfaces, as well as the cover soil and moss horizons. All sites were geolocated using a high-precision RTK GPS system. The field measurement drift was <1%, and selected subsamples remeasured in the lab and were shown to have <3% variation from values obtained in the field. The data campaign also included high-resolution geophysical (70/300 MHz) georadar surveys (Figure 2D), with the ultimate aim of correlating lithostratigraphic units and MS trends with subsurface bounding surfaces.

4. Results

The results of the field measurements are summarized in Table 1 and are presented in Figures 3 and 4. It is worth noting that relative, rather than absolute, MS values need to be considered when comparing trends within each site, both spatially and temporally. The Late Holocene beach ridges at Tahkuna strandplain yielded relatively low MS values with a mean of 4.4 and 4.7 μ SI for ridges TUH-1 (0.7 m deep) and TUH-2 (0.95 m), respectively (Table 1; Figures 2A and 3). The 0.9 m deep trench through the upper, younger section of a ~5 m high parabolic dune had substantially higher susceptibility values, with an average of 68.4 μ SI and maximum of >140 μ SI (Site 5A; Figures 1, 2B and 3).

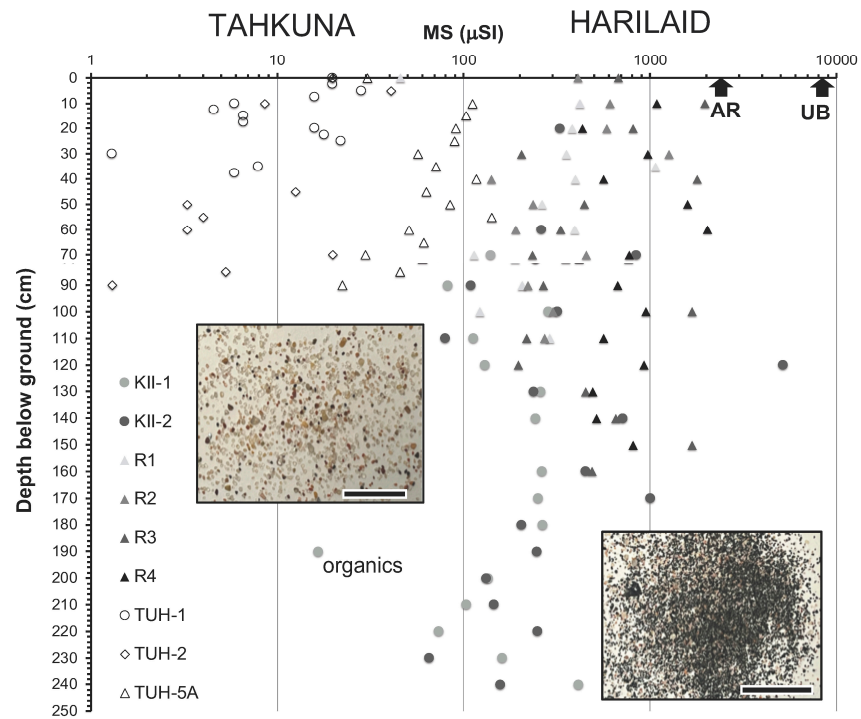


Figure 3. Database of all MS values from the Tahkuna (Hiiumaa) and Harilaid (Saaremaa) sites (logarithmic MS scale). Site names on top reflect the overall pattern as values at Harilaid are 1–2 orders of magnitude greater (mostly >100 μSI), with a low-value outlier representing an organic sample and the highest (>1000 μSI) corresponding to modern beach HMCs and specific intervals in trench/core samples (see Figure 4 for selected vertical and lateral stratigraphic trends). Modern upper-berm (UB) and aeolian ramp (AR) HMCs have unusually high MS values (Table 1) due to bedding plane measurements, in contrast to other points. Insets show medium quartz-rich sand and a slightly finer-grained HMC from an active beach at Harilaid (scale bar = 1 cm).

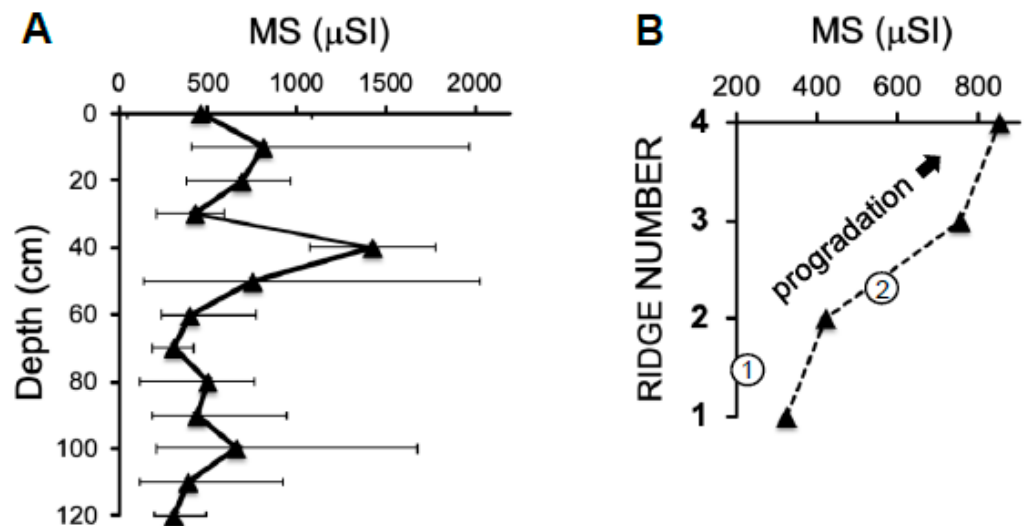


Figure 4. Vertical (trench/core stratigraphic) and lateral (morphostratigraphic) trends. (A) Mean values and ranges of trench and outcrop-based *in situ* MS values from four ridges (R1–R4). Note a well-constrained high MS anomaly at a 0.4 m depth. (B) Mean values of each ridge reveal an increasing trend in a morphostratigraphically younger direction, with the most recent R4 having a >2.5 higher mean MS compared to R1. Two cores (KII-1 and 2) are shown as circles for comparison; however, they have a much greater range of variations due to the presence of both organics and deep HMCs.

The four ridges at Harilaid foreland yielded substantially higher values than Tahkuna (Table 1; Figure 3). The modern beach had the highest MS values, with a very-thin-layer (2–3 mm) cover placer deposit exceeding 8100 μ SI. The modern dunes and aeolian ramp have anomalies with average values of \sim 450 μ SI (Figure 2E). It is worth noting that unusually high MS values of modern subenvironments are largely due to bedding plane measurements, in contrast to trench wall sensor attitude that captures background values from underlying and overlying laminae (Figure 3). In the trenches, cores, and outcrops, many HMC layers exceed 5 mm and show a wide spectrum of bulk MS, with a vast majority in a 100–1000 μ SI range (note the logarithmic scale in Figure 3). An organic-rich (decomposed seaweed) sample in core KII-1 provided the lowest MS of 16.6 μ SI, whereas the highest for a geological sample was an HMC in core KII-2 at 5158.2 μ SI.

Table 1. Bulk low-field magnetic susceptibility (κ , μ SI) values (minimum, maximum, and mean) of 170 sand samples from a suite of morphostratigraphic units and modern subenvironments (see Figure 1 for locations). The context of selected anomalous readings is indicated below, with the majority of MS maxima corresponding to visible heavy mineral concentrations. Note an increase in mean κ through time at Harilaid strandplain (R1 to R4). Buried organics at a 1.9 m depth in core KII-1 (a) yielded low MS values similar to those of the modern swash zones (b). The modern beach (wave-reworked) and dune (wind-transported) samples show that the aeolian ramp (e) along the western scarp (truncated ridge R1) derives its sediment from the HMC-rich upper berm (c). In contrast, the upper part of the scarp and dune top (d) have low values similar to the top of R1.

Location	n	k_{min}	k_{max}	\bar{k}
Tahkuna (n = 68)				
TUH-1	29	−7.3	28.4	4.4
TUH-2 core	20	−3.3	40.9	4.7
TUH-5A	19	0	140.8	68.4
Harilaid (n = 102)				
R1	13	45.7	1069.9	326.6
KII-1 core	17	16.6 ^a	283.7	208.7
R2	12	140.2	1264.3	419.6
KII-2 core	19	65.5	5158.2	561.6
R3	17	195.7	1966.7	754.4
R4	15	415.9	2030.1	851.5
Beach	3	16.9 ^b	8173.1 ^c	2905.4
Dune	6	45.7 ^d	1130.1 ^e	444.4

^a Organics; ^b swash zone; ^c upper berm; ^d dune top; ^e aeolian ramp.

A stratigraphic pattern includes an MS increase in all sections within 0.3–0.6 m below the ridge crest (Figures 2E and 4A). The maximum at 0.4 m is especially well constrained. A second trend is an increase in the average MS values of the four ridge crests with decreasing age (seaward) from \sim 330 to 850 μ SI (ridge R1 and R4, respectively; Table 1; Figure 4B).

5. Discussion and Conclusions

The results of our study show several distinct patterns and highlight the importance of analyzing site-specific trends in relative magnetic susceptibility values from individual cores or trenches to several ridges within a set. Inter-site contrast (between all Tahkuna and Harilaid samples; Table 1) has a greater bearing on the difference in their depositional timeframe. Therefore, each site provides its own pattern of MS trends, and no attempt was made to directly compare them other than to highlight the contrasting ranges of absolute values (Figure 3).

The low values at Tahkuna are due to the dominance of diamagnetic quartz, with minor amounts of felsic feldspar (see inset in Figure 3). This segment of the strandplain formed within the past 2200 years (Figures 1 and 2A) and likely represents a relatively

calm hydroclimatic regime (Tõnisson et al., 2018). The parabolic dune likely formed ~800 yBP as a result of the reworking of beach ridge segments seaward of beach ridges 1 and 2 [29]. Such dunes often provide an independent archive of wind stress related to coastal storms [1–4,12,30–34]. Future research is planned along the seaward sections of Tahkuna strandplain to see how they compare to the much higher values found at the Harilaid site on Saaremaa.

At the Harilaid foreland, the magnetite fraction is the primary cause of magnetic susceptibility values, with other paramagnetic minerals (e.g., almandine garnet, ilmenite, and amphiboles; see inset in Figure 3) causing additional MS increases [35–38]. Thin, high-value anomalies can be potentially used to locate the beach dune boundary, with further research needed. This can be accomplished by comparing the depth of such an anomaly with a georadar signature of the upper berm: (1) flattening of seaward-dipping clinoforms or (2) transition between the sub-horizontal (berm) and chaotic (foredune) bounding surfaces [5,39–41].

Thick heavy mineral concentrations, similar to those at Harilaid, often accompany morphological signatures of beach and dune sections that have undergone storm reworking [7,8,10,42,43]. These can be identified in trenches and GPR images as strong (high-amplitude) seaward-dipping sub-horizontal reflections of eroded beach faces and/or steep disconformities that truncate paleo-berm (berm scarp) or dune (dune scarp) bounding surfaces [9,11,39,42,44,45]. Such efforts are underway for images collected during MS surveys (Figure 2D) and will be the focus of future publications. An additional aspect of HMCs, even thin horizons, is their potential adverse influence on optically stimulated luminescence dating (OSL) results [39]. Thus, the strategy for selecting intervals for OSL sampling can be easily guided by MS measurements in trenches and outcrops (Figure 2E) selected for chronological control, as was the case in this study.

Such integrated datasets of textural, MS, chronological, and high-resolution geophysical data are revolutionizing coastal research in sand-dominated sequences that have been challenging to study using traditional geological techniques. For example, the granulometric analysis of HMC-quartz couplets that may be a result of deposition during the waning stages of a storm will often show a reverse grading. Hydrodynamically, however, the finer-grained heavy mineral fraction is coarser due to surface area/volume considerations and dispersive pressure effects [7,10,46–48]. When grain size data are “normalized” using MS values, which are a function of both density and particle size, a more accurate picture can be obtained and included in the quantitative analysis of shear stress.

It is possible that MS peaks at 30–60 cm depths below each ridge crest (Figure 4A) may be due to the acceleration of near-surface wind due to vertical ridge growth (aggradation), with capping sediment representing a cessation in wind activity and initiation of vegetation. Alternatively, there may be a pedogenic component to such HMC trends, although it is present in ridges of varying ages. A trend of a progressive mean MS increases from older to younger sites (R1–R4; Table 1; Figure 4B) may be related to either (1) a temporal increase in the overall energy of the aero/hydrodynamic agents during deposition or (2) changes in the sediment source with a finite fraction of heavy minerals (primarily magnetite). Such trends may potentially serve for intra-site (along a single ridge) or inter-site (coeval ridges) morphostratigraphic correlations.

Recent research on Estonian strandplains [6,49–51] proposes a climatically mediated cyclicality, with major ridge sets and morphostratigraphic discontinuities likely related to storm periods. Ultimately, such patterns may be linked to hemisphere-scale perturbations in North Atlantic Oscillation or related phenomena, with Estonia being the easternmost coastal region in this system [29,52].

Our dataset will be compared to other paleotempestological proxies, such as clastic flux in coastal wetlands [53], to investigate a potential for an integrated erosional–depositional regional database for intense historic and prehistoric events. Furthermore, localized HMC anomalies have the potential to reveal past tracking surfaces of paleo-ecological and archaeological significance by accentuating footprints on otherwise monotonous aeolian bedding

planes [12,14,21,54]. This study demonstrates that the low-field MS methodology presented here has high potential to complement ongoing and future research along the Baltic coastal sequences in Lithuania, Latvia, and Estonia and will serve as valuable lithostratigraphic and paleo-energy indicators.

Author Contributions: Conceptualization, I.V.B. and H.T.; methodology, I.V.B.; software, I.V.B.; validation, I.V.B., H.T.; formal analysis, I.V.B.; investigation, I.V.B., H.T., T.T., A.R., T.H., S.S., A.K., V.P. and S.F.S.D.; resources, H.T.; data curation, I.V.B.; writing—original draft preparation, I.V.B.; writing—review and editing, I.V.B., A.R., T.H., A.K.; visualization, I.V.B.; supervision, I.V.B. and H.T.; project administration, H.T.; funding acquisition, I.V.B. and H.T. All authors have read and agreed to the published version of the manuscript.

Funding: This research was funded by [Estonian Research Council Grants] and [the College of Science and Technology (Temple University, USA)], grant number [IUT18-9 and PRG1471]. And The APC was funded by [Estonian Research Council Grants] and [the College of Science and Technology (Temple University, USA)].

Institutional Review Board Statement: Not applicable.

Informed Consent Statement: Not applicable.

Data Availability Statement: Not applicable.

Acknowledgments: We thank the people of Hiiumaa and Saaremaa for their hospitality during field research.

Conflicts of Interest: The authors declare no conflict of interest.

References

1. Clemmensen, L.B.; Andreassen, F.; Heinemeier, J.; Murray, A. A Holocene coastal aeolian system, Vejers, Denmark: Landscape evolution and sequence stratigraphy. *Terra Nova* **2001**, *13*, 129–134. [\[CrossRef\]](#)
2. Clarke, M.L.; Rendell, H.M.; Tastet, J.-P.; Clavé, B.; Massé, L. Late-Holocene sand invasion and North Atlantic storminess along the Aquitaine Coast, southwest France. *Holocene* **2002**, *12*, 231–238. [\[CrossRef\]](#)
3. Clarke, M.L.; Rendell, H.M. Effects of storminess, sand supply and the North Atlantic Oscillation on sand invasion and coastal dune accretion in western Portugal. *Holocene* **2006**, *16*, 341–355. [\[CrossRef\]](#)
4. Buynevich, I.V.; Bitinas, A.; Pupienis, D. Lithological anomalies in a relict coastal dune: Geophysical and paleoenvironmental markers. *Geophys. Res. Lett.* **2007**, *34*, L09707. [\[CrossRef\]](#)
5. Tamura, T. Beach ridges and prograded beach deposits as palaeoenvironment records. *Earth Sci. Rev.* **2012**, *114*, 279–297. [\[CrossRef\]](#)
6. Suursaar, Ü.; Rosentau, A.; Hang, T.; Tõnisson, H.; Tamura, T.; Vaasma, T.; Vandel, E.; Vilumaa, K.; Sugita, S. Climatically induced cyclicity recorded in the morphology of uplifting Tihu coastal ridgeplain, Hiiumaa Island, eastern Baltic Sea. *Geomorphology* **2022**, *404*. [\[CrossRef\]](#)
7. Komar, P.D.; Wang, C. Processes of selective grain transport and the formation of placers on beaches. *J. Geol.* **1984**, *92*, 637–655. [\[CrossRef\]](#)
8. Smith, A.W.; Jackson, L.A. Assessment of the past extent of cyclone beach erosion. *J. Coast. Res.* **1990**, *6*, 73–86.
9. Dougherty, A.J.; FitzGerald, D.M.; Buynevich, I.V. Evidence for storm-dominated early progradation of Castle Neck Barrier, Massachusetts, USA. *Mar. Geol.* **2004**, *210*, 123–134. [\[CrossRef\]](#)
10. Kattaa, B. Heavy mineral survey of the Syrian beach sands, south of Tartous: Their nature, distribution and potential. *Explor. Min. Geol.* **2004**, *11*, 31–41. [\[CrossRef\]](#)
11. Van Dam, R.L.; Hendrickx, J.M.H.; Cassidy, N.J.; North, R.E.; Dogan, M.; Borchers, B. Effects of magnetite on high-frequency ground-penetrating radar. *Geophysics* **2013**, *78*, H1–H11. [\[CrossRef\]](#)
12. Buynevich, I.V. Morphologically induced density lag formation on bedforms and biogenic structures in aeolian sands. *Aeolian Res.* **2012**, *7*, 11–15. [\[CrossRef\]](#)
13. Pupienis, D.; Buynevich, I.V.; Ryabchuk, D.; Jarmalavičius, D.; Žilinskas, G.; Fedorovič, J.; Kovaleva, O.; Sergeev, A.; Cichoń-Pupienis, A. Spatial patterns in heavy-mineral concentrations along the Curonian Spit coast, southeastern Baltic Sea. *Estuar. Coast. Shelf Sci.* **2017**, *195*, 41–50. [\[CrossRef\]](#)
14. Buynevich, I.V. Detection of mineralogically accentuated biogenic structures with high-resolution geophysics: Implications for ichnology and geoecology. *J. Geol. Geogr. Geoecol.* **2020**, *29*, 252–257. [\[CrossRef\]](#)
15. Vassiljev, J.; Saarse, L.; Grudzinska, I.; Heinsalu, A. Relative sea level changes and development of the Hiiumaa Island, Estonia, during the Holocene. *Geol. Quat.* **2015**, *59*, 517–530. [\[CrossRef\]](#)

16. Rosentau, A. and 28 co-authors. A Holocene relative sea-level database for the Baltic Sea. *Quat. Sci. Rev.* **2021**, *266*, 107071. [[CrossRef](#)]
17. Nirgi, T.; Grudzinska, I.; Kalińska, E.; Konsa, M.; Jõelett, A.; Alexanderson, H.; Hang, T.; Rosentau, A. Late-Holocene relative sea-level changes and palaeoenvironment of the Pre-Viking Age ship burials in Salme, Saaremaa Island, eastern Baltic Sea. *Holocene* **2022**, *32*, 237–253.
18. Kont, A.; Ratas, U.; Puurmann, E. Sea-level rise impact on coastal areas of Estonia. *Clim. Chang.* **1997**, *36*, 175–184.
19. Kriiska, A.; Hang, T.; Rosentau, A. Palaeogeographic model for the SW Estonian coastal zone of the Baltic Sea. In *The Baltic Sea Basin (Central and Eastern European Development Studies)*; Harff, J., Bjorck, S., Hoth, P., Eds.; Springer: Berlin/Heidelberg, Germany, 2011; pp. 165–188.
20. Vilumaa, K.; Ratas, U.; Tõnisson, H.; Kont, A.; Pajula, R. Multidisciplinary approach to studying the formation and development of beach-ridge systems on non-tidal uplifting coasts in Estonia. *Boreal Env. Res.* **2017**, *22*, 67–81.
21. Muru, M.; Rosentau, A.; Preusser, F.; Plado, J.; Sibul, I.; Jõelett, A.; Bjursäter, S.; Aunap, R.; Kriiska, A. Reconstructing Holocene shore displacement and Stone Age palaeogeography from a foredune sequence on Ruhnu Island, Gulf of Riga, Baltic Sea. *Geomorphology* **2018**, *303*, 434–445. [[CrossRef](#)]
22. Ravis, R.; Ratas, U.; Kont, A. Some Implications of Coastal Processes Associated with Climate Change on Harilaid, Western Estonia. In *Proceedings of the Littoral 2002. 6th International Symposium: The Changing Coast, Porto, Portugal, 22–26 September 2002*; pp. 133–139.
23. Orviku, K.; Suursaar, Ü.; Tõnisson, H.; Kullas, T.; Ravis, R.; Kont, A. Coastal changes in Saaremaa Island, Estonia, caused by winter storms in 1999, 2001, 2005 and 2007. *J. Coast. Res.* **2009**, *SI56*, 1651–1655.
24. Orviku, K.; Tõnisson, H.; Jaagus, J. Sea ice shaping the shores. *J. Coast. Res.* **2011**, *SI64*, 681–685.
25. Suursaar, Ü.; Jaagus, J.; Kont, A.; Ravis, R.; Tõnisson, H. Field observations on hydrodynamic and coastal geomorphic processes off Harilaid Peninsula (Baltic Sea) in winter and spring 2006–2007. *Estuar. Coast. Shelf Sci.* **2008**, *80*, 31–41. [[CrossRef](#)]
26. Soomere, T.; Behrens, A.; Tuomi, L.; Nielsen, J.W. Wave conditions in the Baltic proper and in the Gulf of Finland during windstorm Gudrun. *Nat. Hazards Earth Syst. Sci.* **2008**, *8*, 37–46. [[CrossRef](#)]
27. Tõnisson, H.; Orviku, K.; Jaagus, J.; Suursaar, Ü.; Kont, A.; Ravis, R. Coastal damages on Saaremaa Island, Estonia, caused by the extreme storm and flooding on January 9, 2005. *J. Coast. Res.* **2008**, *24*, 602–614. [[CrossRef](#)]
28. Tõnisson, H.; Suursaar, Ü.; Ravis, R.; Kont, A.; Orviku, K. Observation and analysis of coastal changes in the West Estonian Archipelago caused by storm Ulli (Emil) in January 2012. *J. Coast. Res.* **2013**, *SI65*, 832–837. [[CrossRef](#)]
29. Tõnisson, H.; Suursaar, Ü.; Kont, A.; Muru, M.; Ravis, R.; Rosentau, A.; Tamura, T.; Vilumaa, K. Rhythmic patterns of coastal formations as signs of past climate fluctuations on uplifting coasts of Estonia, the Baltic Sea. *J. Coast. Res.* **2018**, *SI85*, 611–615. [[CrossRef](#)]
30. Seppälä, M. Deflation and redeposition of sand dunes in Finnish Lapland. *Quat. Sci. Rev.* **1995**, *14*, 799–809. [[CrossRef](#)]
31. Lancaster, N. Response of eolian geomorphic systems to minor climate change: Examples from the southern Californian deserts. *Geomorphology* **1997**, *19*, 333–347. [[CrossRef](#)]
32. Botha, G.A.; Bristow, C.S.; Porat, N.; Duller, G.; Armitage, S.J.; Roberts, H.M.; Clarke, B.M.; Kota, M.W.; Schoeman, P. Evidence for dune reactivation from GPR profiles on the Mputuland coastal plain, South Africa. In *Ground Penetrating Radar in Sediments*; Bristow, C.S., Jol, H.M., Eds.; Geological Society: London, UK, 2003; Volume 211, pp. 29–46.
33. Habicht, H.-L.; Rosentau, A.; Jõelett, A. GIS-based multiproxy coastline reconstruction of the eastern gulf of Riga, Baltic Sea, during the stone age. *Boreas* **2017**, *46*, 83–99. [[CrossRef](#)]
34. Tõnisson, H.; Suursaar, Ü.; Ravis, R.; Tamura, T.; Aarna, T.; Vilumaa, K.; Kont, A. Characteristics and formation of a solitary dune belt encountered along the coast of Estonia. *J. Coast. Res.* **2020**, *SI95*, 689–694. [[CrossRef](#)]
35. Raukas, A.; Bird, E.D.; Orviku, K. The provenance of beaches on the Estonian islands of Hiiu and Saaremaa. *Proc. Est. Acad. Sci. Geol.* **1994**, *43*, 81–92.
36. Raukas, A.; Koch, R.; Juriado, K.; Järvelill, J.I. Anomalous radioactivity level and high concentrations of heavy minerals in Lemme area, South-West Estonia. *Baltica* **2014**, *27*, 93–104. [[CrossRef](#)]
37. Shankar, R.; Thompson, R.; Prakash, T.N. Estimation of heavy and opaque mineral contents of beach and offshore placers using rock magnetic techniques. *Geo. Mar. Lett.* **1996**, *16*, 313–318. [[CrossRef](#)]
38. Järvelill, J.-I.; Kleesment, A.; Raukas, A. Accumulation of heavy minerals in the eastern coast of the Gulf of Riga, south-western Estonia. *Bull. Geol. Soc. Finl.* **2015**, *87*, 67–78. [[CrossRef](#)]
39. Buynevich, I.V.; FitzGerald, D.M.; Goble, R.J. A 1500-year record of North Atlantic storm activity based on optically dated relict beach scarps. *Geology* **2007**, *35*, 543–546. [[CrossRef](#)]
40. Buynevich, I.V.; Jol, H.M.; FitzGerald, D.M. Coastal Environments. In *Ground Penetrating Radar: Theory and Applications*; Jol, H.M., Ed.; Elsevier: Amsterdam, The Netherlands, 2009; pp. 299–322.
41. van Heteren, S.; FitzGerald, D.M.; McKinlay, P.A.; Buynevich, I.V. Radar facies of paraglacial barrier systems: Coastal New England, USA. *Sedimentology* **1998**, *45*, 181–200. [[CrossRef](#)]
42. Buynevich, I.V.; FitzGerald, D.M.; van Heteren, S. Sedimentary records of intense storms in Holocene barrier sequences, Maine, USA. *Mar. Geol.* **2004**, *210*, 135–148. [[CrossRef](#)]
43. Buynevich, I.V.; Kadurin, S.V. Paleo-storm indicators within Sasyk Liman baymouth barrier, Ukraine. *Geol. Bull. Lviv Natl. Univ. Ukr.* **2015**, *i*, 53–59.

44. Rosentau, A.; Jõelett, A.; Plado, J.; Aunap, R.; Muru, M.; Eskola, K.O. Development of the Holocene foredune plain in the Narva-Jõesuu area, eastern Gulf of Finland. *Geol. Q.* **2013**, *57*, 89–100.
45. Vilumaa, K.; Tõnisson, H.; Sugita, S.; Buynevich, I.V.; Kont, A.; Muru, M.; Preusser, F.; Bjursäter, S.; Vaasma, T.; Vandel, E.; et al. Past extreme events recorded in the internal architecture of coastal formations in the Baltic Sea region. *J. Coast. Res.* **2016**, *SI75*, 775–779. [[CrossRef](#)]
46. Komar, P.D. Physical processes of waves and currents and the formation of marine placers. *Rev. Aquat. Sci.* **1989**, *1*, 393–423.
47. Hughes, M.G.; Keene, J.B.; Joseph, R.G. Hydraulic sorting of heavy-mineral grains by swash on a medium-sand beach. *J. Sediment. Res.* **2000**, *70*, 994–1004. [[CrossRef](#)]
48. Tomkins, M.R.; Nielsen, P.; Michael, G.; Hughes, M.G. Selective entrainment of sediment graded by size and density under waves. *J. Sediment. Res.* **2003**, *73*, 906–911. [[CrossRef](#)]
49. Suursaar, Ü.; Tõnisson, H. Storminess-related rhythmic ridge patterns on the coasts of Estonia. *Estonian J. Earth Sci.* **2017**, *66*, 220–237. [[CrossRef](#)]
50. Suursaar, Ü.; Kall, T.; Steffen, H.; Tõnisson, H. Cyclicity in ridge patterns on the prograding coasts of Estonia. *Boreas* **2019**, *48*, 913–928. [[CrossRef](#)]
51. Suursaar, Ü.; Jaagus, J.; Tõnisson, H. How to quantify long-term changes in coastal sea storminess? *Estuar. Coast. Shelf Sci.* **2015**, *156*, 31–41. [[CrossRef](#)]
52. Tõnisson, H.; Suursaar, Ü.; Orviku, K.; Jaagus, J.; Kont, A.; Willis, D.A.; Ravis, R. Changes in coastal processes in relation to changes in large-scale atmospheric circulation, wave parameters and sea levels in Estonia. *J. Coast. Res.* **2011**, *SI64*, 701–705.
53. Vandel, E.; Vaasma, T.; Sugita, S.; Tõnisson, H.; Jaagus, J.; Vilumaa, K.; Anderson, A.; Kont, A. Reconstruction of past storminess: Evaluation of an indicator approach using aeolian mineral grains buried in peat deposits, Estonia. *Quat. Sci. Rev.* **2019**, *218*, 215–227. [[CrossRef](#)]
54. Rosentau, A.; Nirgi, T.; Muru, M.; Bjursäter, S.; Hang, T.; Preusser, F.; Risberg, J.; Sohar, K.; Tõnisson, H.; Kriiska, A. Holocene relative shore level changes and Stone Age hunter-gatherers in Hiiumaa Island, eastern Baltic Sea. *Boreas* **2020**, *49*, 783–798. [[CrossRef](#)]

Disclaimer/Publisher's Note: The statements, opinions and data contained in all publications are solely those of the individual author(s) and contributor(s) and not of MDPI and/or the editor(s). MDPI and/or the editor(s) disclaim responsibility for any injury to people or property resulting from any ideas, methods, instructions or products referred to in the content.